Alloying Sb into all inorganic lead-free $CsBi_3I_{10}$ for improving the crystal growth and photovoltaic performance

*Jian Kang,[a] Shan Chen,[*b] Mengmeng Hao,[d] Junxian Liu,[a] Mohammad Al-Mamun,[a] Porun Liu,[a] Yun Wang,[a] Huajie Yin,[*c] and Huijun Zhao[*a]*

a. Centre for Catalysis and Clean Energy, School of Environment and Science, Griffith University, Gold Coast, QLD 4222, Australia
b. Institutes of Physical Science and Information Technology, Anhui University, Hefei, 230039, China
c. Institute of Solid-State Physics, Chinese Academy of Sciences, Hefei, 230031, China
d. School of Chemical Engineering and Australian Institute of Bioengineering and Nanotechnology, The University of Queensland, Brisbane, QLD 4072, Australia

*Corresponding author. E-mail: h.zhao@griffith.edu.au; chenshan@ahu.edu.cn; yinhj@issp.ac.cn.

Table S1. Photovoltaic performance of $Cs(Bi_xSb_{1-x})_3I_{10}$ devices prepared from DMF and DMSO mixed solvent with volume ratio of 9:1.

Sample	V_{oc} (V)	J_{sc} (mA cm^{-2})	FF (%)	PCE (%)
$CsBi_3I_{10}$	0.47	2.55	38.7	0.45
$Cs(Bi_{0.7}Sb_{0.3})_3I_{10}$	0.74	2.57	32.6	0.62
$Cs(Bi_{0.5}Sb_{0.5})_3I_{10}$	0.65	0.99	25.6	0.16

Table S2. Photovoltaic performance of $Cs(Bi_{0.7}Sb_{0.7})_3I_{10}$ devices prepared from mixed DMF/DMSO solvents with different DMSO volume ratios.

DMSO concentration	V_{oc} (V)	J_{sc} (mA cm^{-2})	FF (%)	PCE (%)
0%	0.69	0.52	27.9	0.10
30%	0.72	3.50	31.7	0.80
50%	0.72	3.93	32.5	0.92
100%	0.75	4.62	30.7	1.06

Table S3. Photovoltaic performance of $Cs(Bi_xSb_{1-x})_3I_{10}$ devices prepared from 100 vol% DMSO solvent.

x (Sb content)	V_{oc} (V)	J_{sc} (mA cm^{-2})	FF (%)	PCE (%)
0	0.46	2.89	41.8	0.55
0.1	0.54	1.26	30.8	0.21
0.2	0.63	2.50	29.2	0.46
0.25	0.73	3.21	30.7	0.72
0.3	0.75	4.62	30.7	1.06
0.35	0.75	4.24	30.2	0.96
0.4	0.75	4.18	29.0	0.91

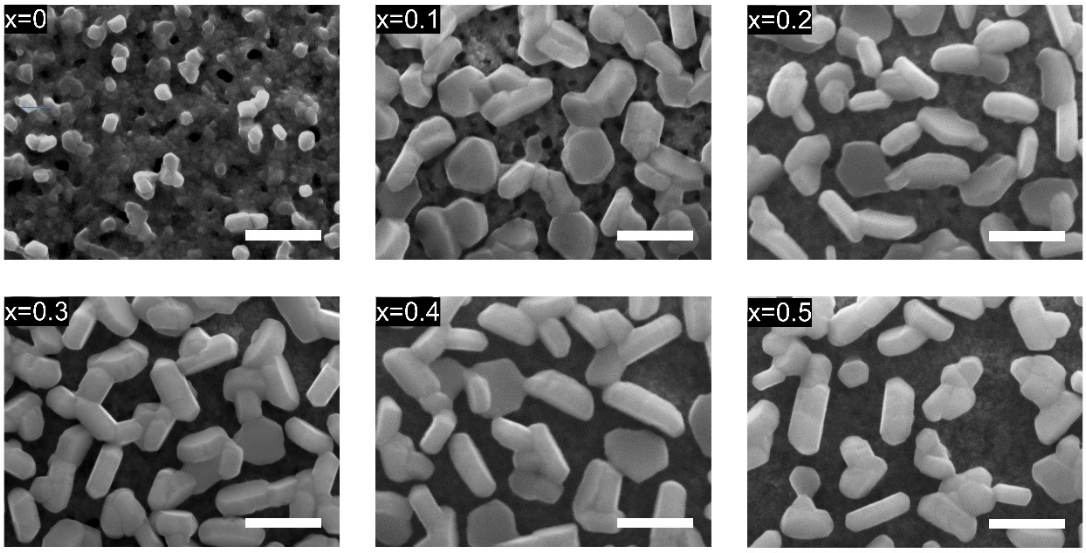

Fig. S1. SEM images of $Cs(Bi_{1-x}Sb_x)_3I_{10}$ films (x=0, 0.1, 0.2, 0.3, 0.4, 0.5) from DMF/DMSO (9:1 v/v) solvent. (Scale bar: 500 nm)

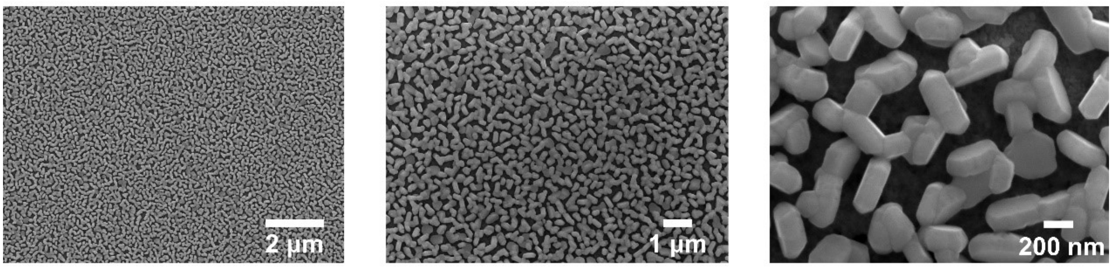

Fig. S2. SEM images of $Cs(Bi_{0.7}Sb_{0.3})_3I_{10}$ film from different scanning scales.

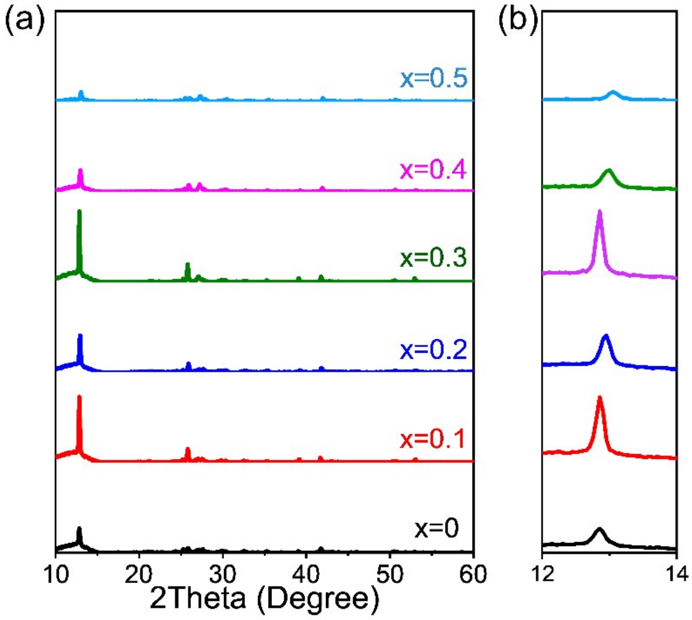

Fig. S3. XRD patterns of $Cs(Bi_{1-x}Sb_x)_3I_{10}$ thin films (x = 0, 0.1, 0.2, 0.3, 0.4, 0.5).

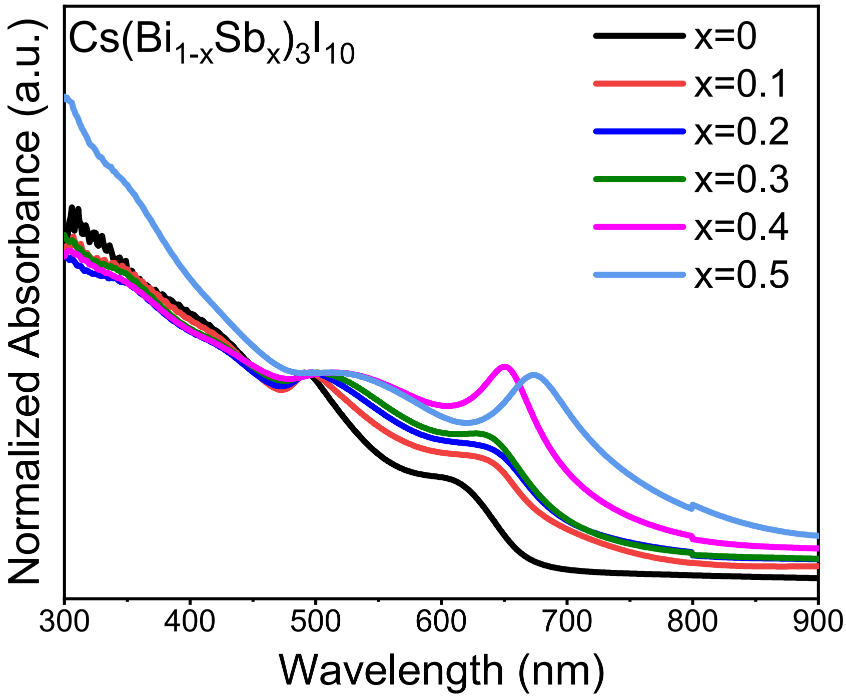

Fig. S4. Uv-vis absorbance spectra of $Cs(Bi_{1-x}Sb_x)_3I_{10}$ thin films (x = 0, 0.1, 0.2, 0.3, 0.4, 0.5).

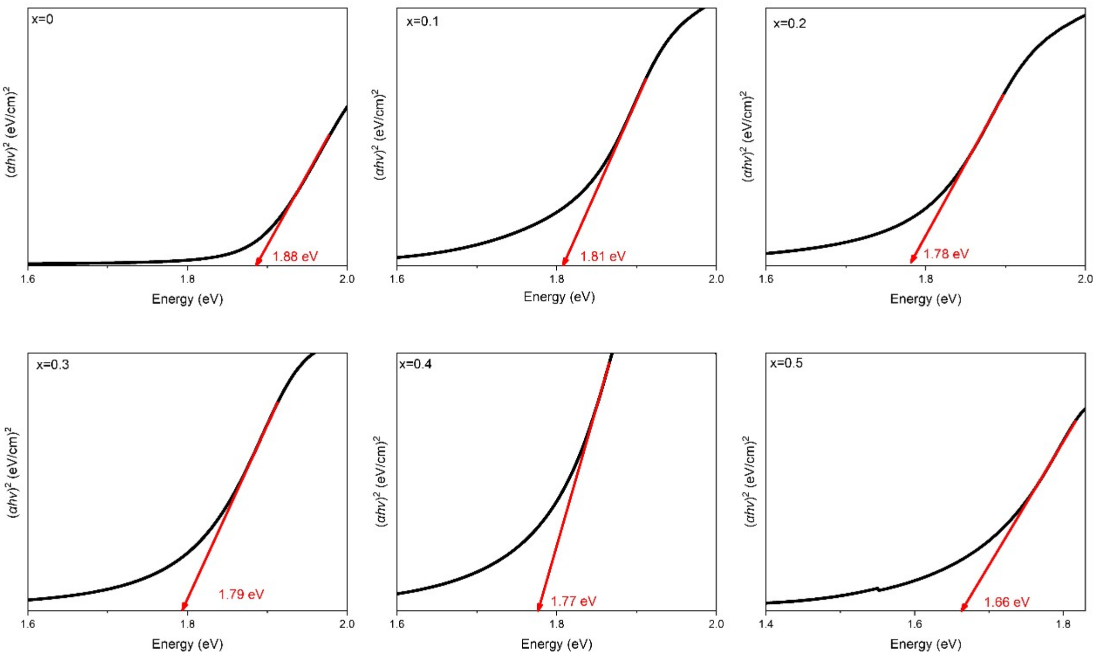

Fig. S5. Tauc-plots derived from optical absorbance of $Cs(Bi_{1-x}Sb_x)_3I_{10}$ thin films (x = 0, 0.1, 0.2, 0.3, 0.4, 0.5) assuming direct transition.

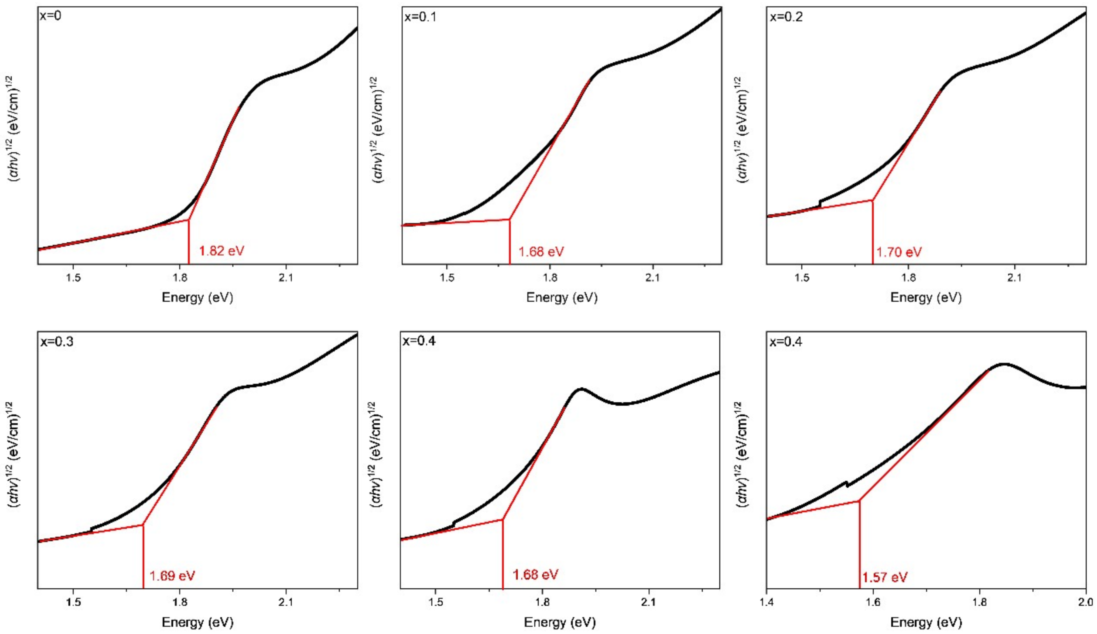

Fig. S6. Tauc-plots derived from optical absorbance of $Cs(Bi_{1-x}Sb_x)_3I_{10}$ thin films (x = 0, 0.1, 0.2, 0.3, 0.4, 0.5) assuming indirect transition.

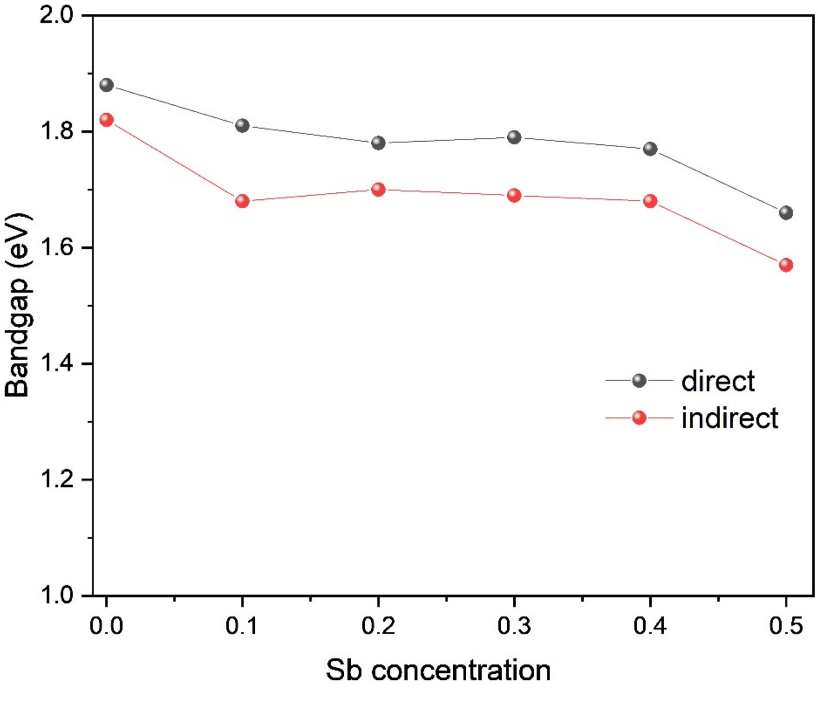

Fig. S7. Calculated bandgaps vs different Sb-substitution ratios.

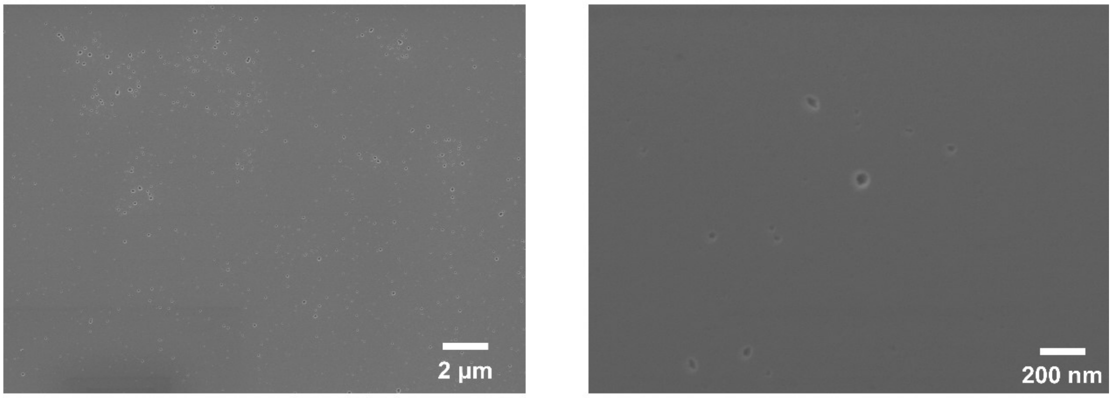

Fig. S8. SEM images of $Cs(Bi_{0.7}Sb_{0.3})_3I_{10}$ film from pure 100 vol% DMF solvent.

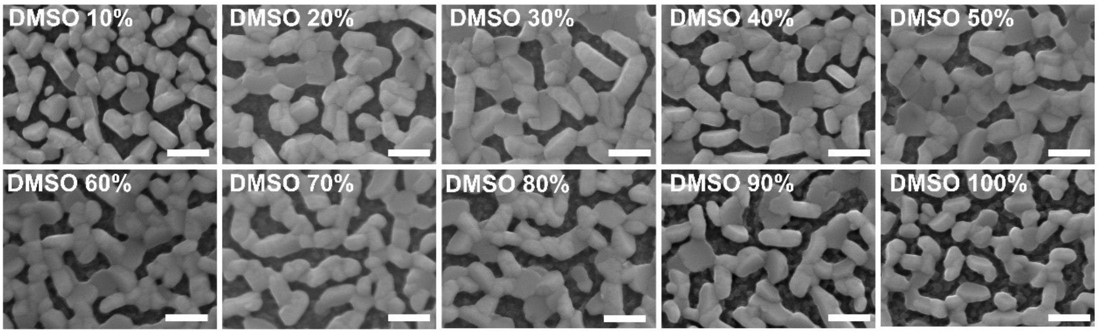

Fig. S9. SEM images of $Cs(Bi_{0.7}Sb_{0.3})_3I_{10}$ films from solvents with different DMSO volume ratios. (Scale bar: 500 nm)

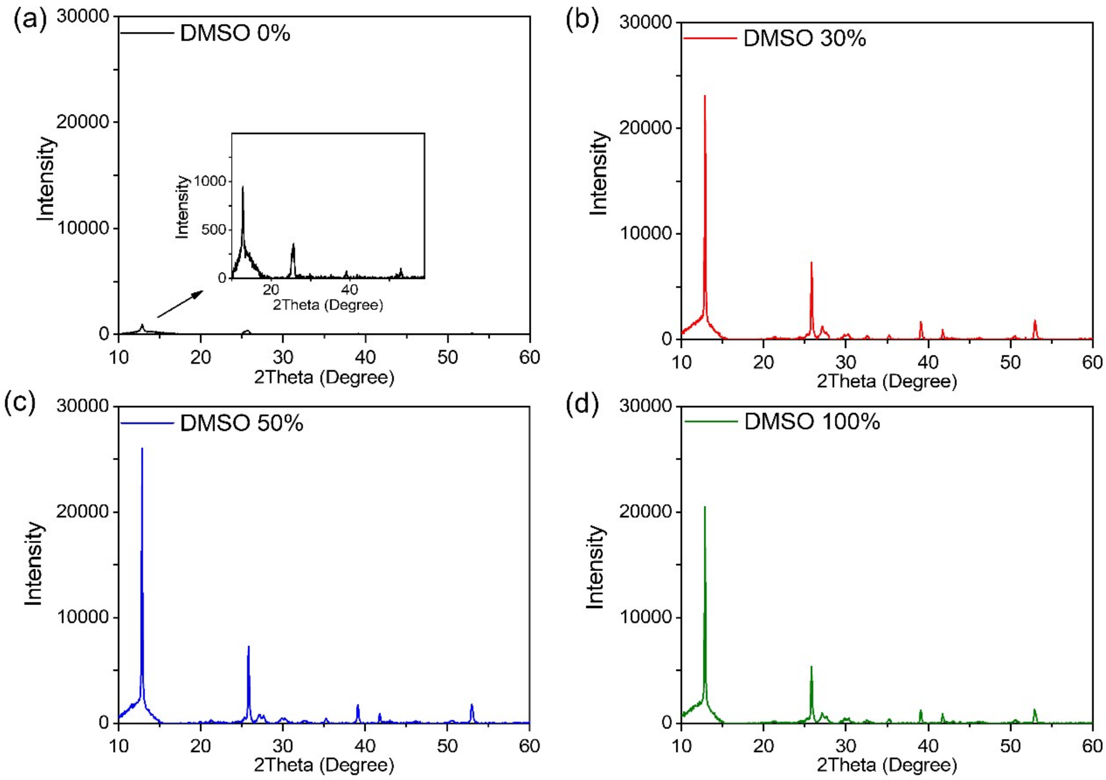

Fig. S10. XRD patterns of $Cs(Bi_{0.7}Sb_{0.3})_3I_{10}$ films synthesized from solvents with different DMSO volume ratios.

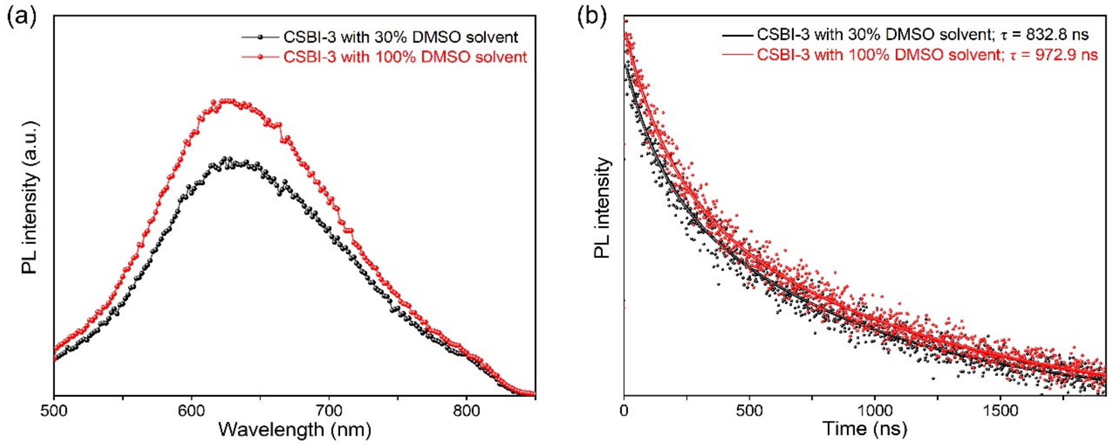

Fig. S11. Steady-state PL (a) and time resolved PL (TRPL) (b) spectra of CBSI-3 films prepared from low-DMSO-contained solvent (DMSO 30 vol%) and high-DMSO-contained solvent (DMSO 100 vol%).

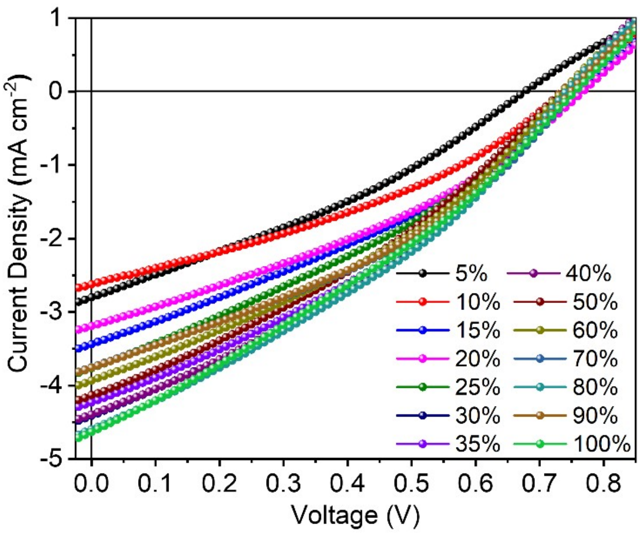

Fig. S12. J-V plots of $Cs(Bi_{0.7}Sb_{0.3})_3I_{10}$ devices from solvents with different DMSO volume ratios with the device structure of ITO/PEDOT/CBSI-3/PCBM/BCP/Ag.

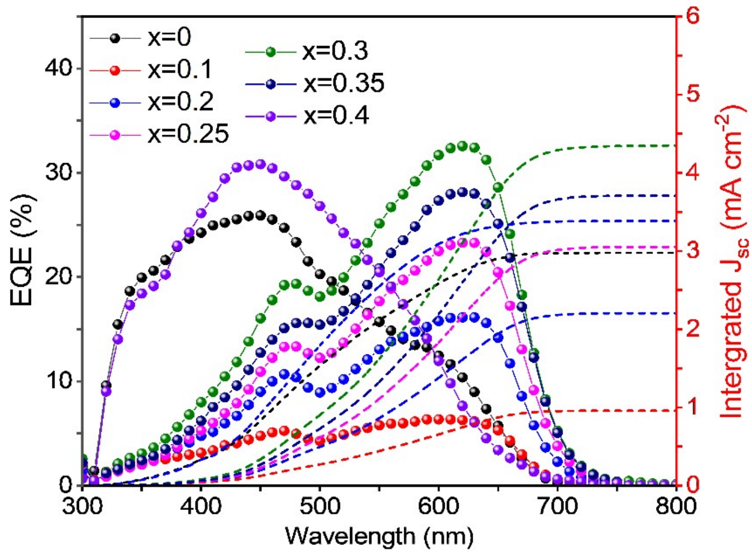

Fig. S13. EQE curves of $Cs(Bi_{1-x}Sb_x)_3I_{10}$ solar cells from 100 vol% DMSO solvent with the structure of ITO/PEDOT/CSBI/PCBM/BCP/Ag.

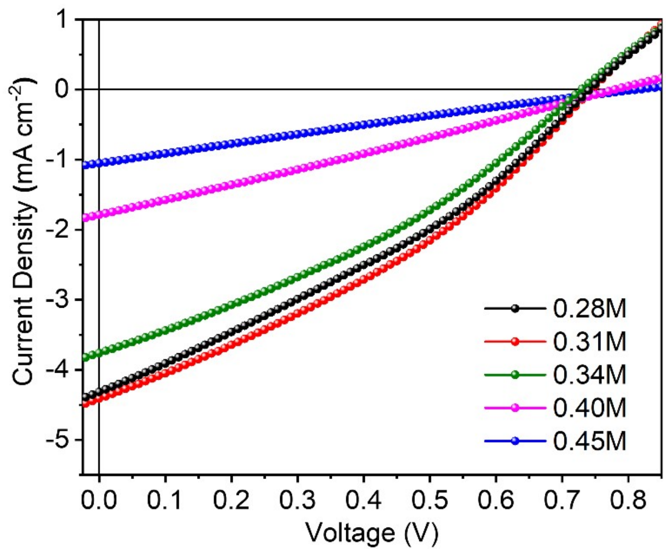

Fig. S14. J-V plots of $Cs(Bi_{0.7}Sb_{0.3})_3I_{10}$ devices from different precursor solution concentrations, and CSBI-3 films here were synthesized from 100 vol% DMSO solvent.

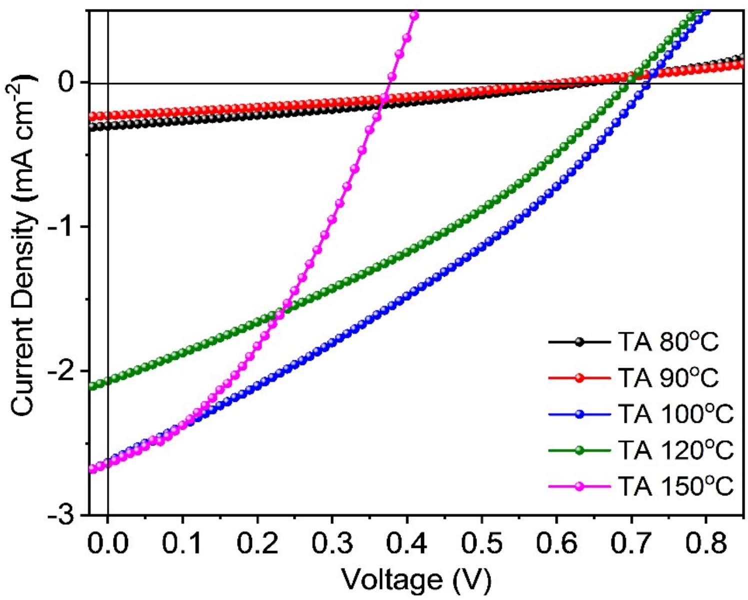

Fig. S15. J-V plots of $Cs(Bi_{0.7}Sb_{0.3})_3I_{10}$ solar cells with CSBI-3 films being synthesized from DMF/DMSO mixed solvent with volume ratio of 9:1 and post-annealed at different temperatures.

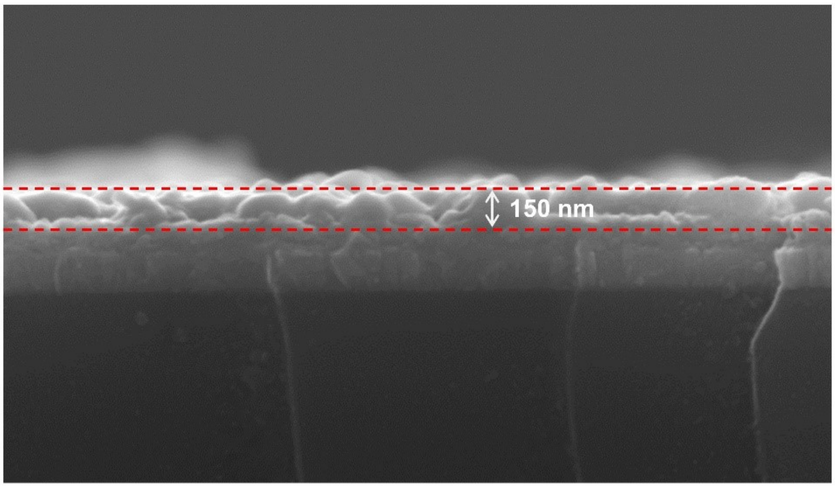

Fig. S16. Cross-sectional SEM image of $Cs(Bi_{0.7}Sb_{0.3})_3I_{10}$/PCBM heterojuntion film as the active layer on the ITO/PEDOT substrate. The $Cs(Bi_{0.7}Sb_{0.3})_3I_{10}$ film was synthesized from 0.31 M precursor solution using pure 100 vol% DMSO as solvent.

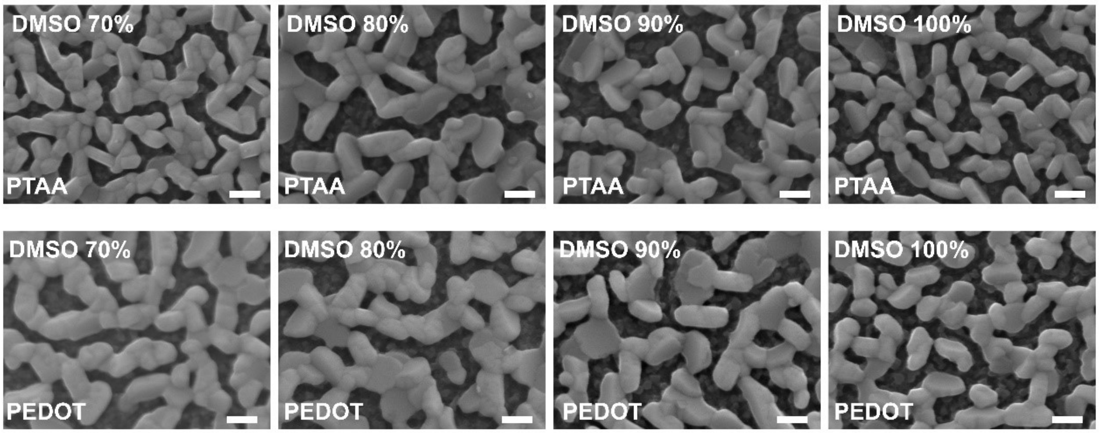

Fig. S17. SEM images of $Cs(Bi_{0.7}Sb_{0.3})_3I_{10}$ films on PTAA and PEDOT substrates with different DMSO volume ratios. (Scale bar: 300 nm)

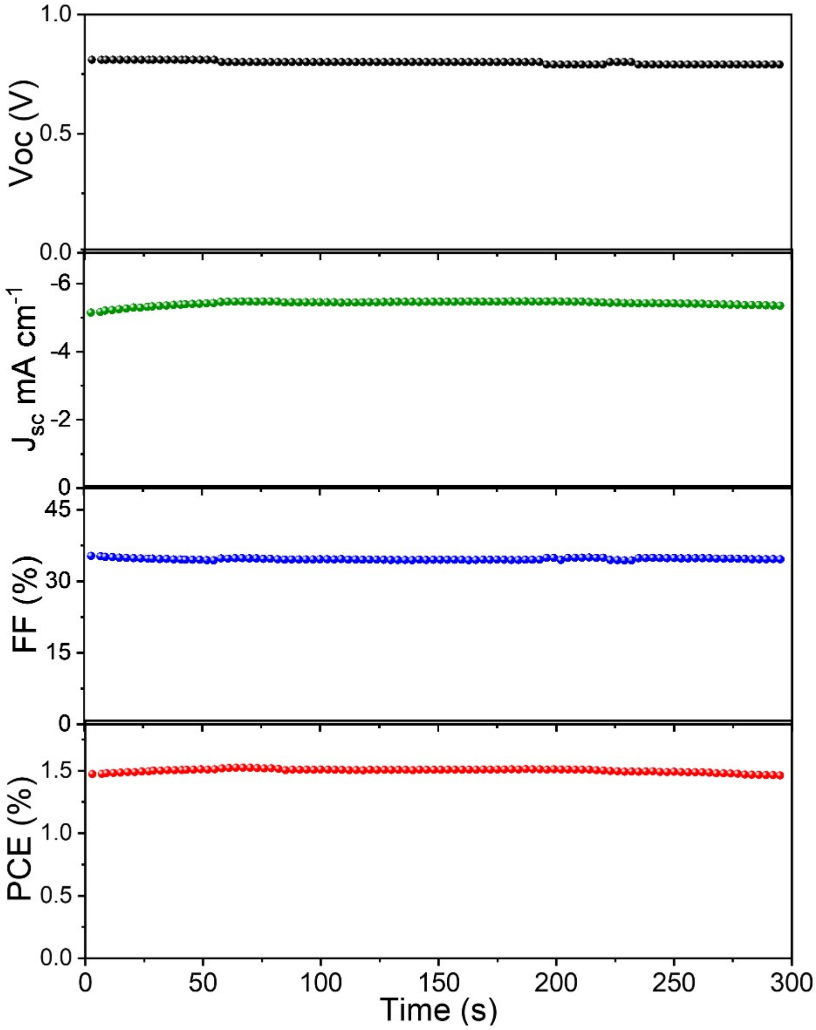

Fig. S18. Power output tracking by continuous measuring the *J-V* curves in air under ambient conditions.

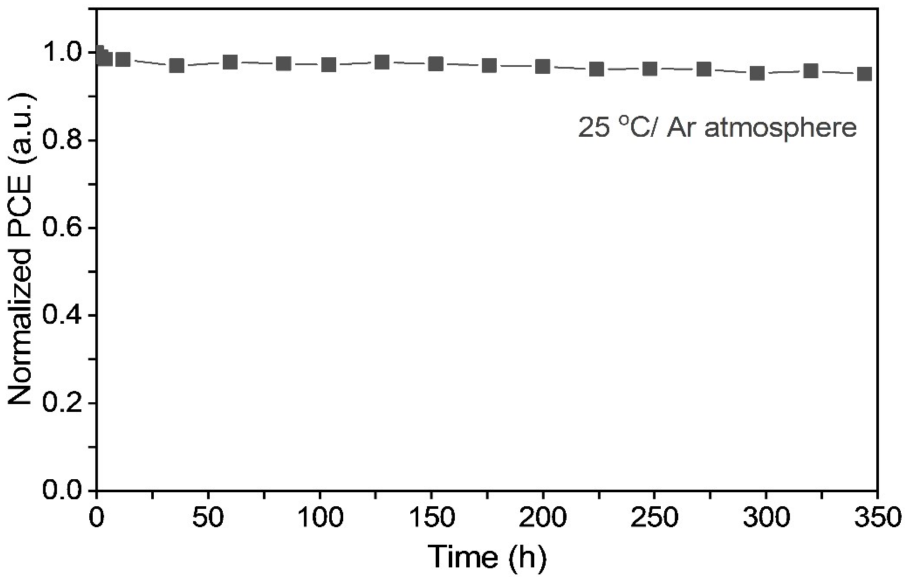

Fig. S19. Storage stability of CSBI-3 solar cell tested over a 14-day period in an Ar-filled glovebox.

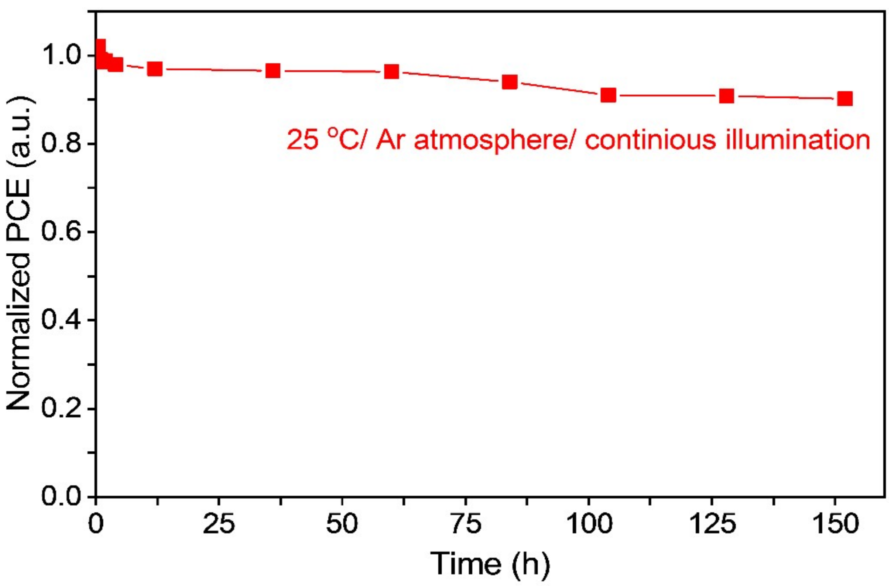

Fig. S20. Light-soaking stability of CSBI-3 solar cell tested over a 7-day period in an Ar-filled glovebox.